Volume 47, Number 3 July, 2023

# Technical Soaring

## An International Journal

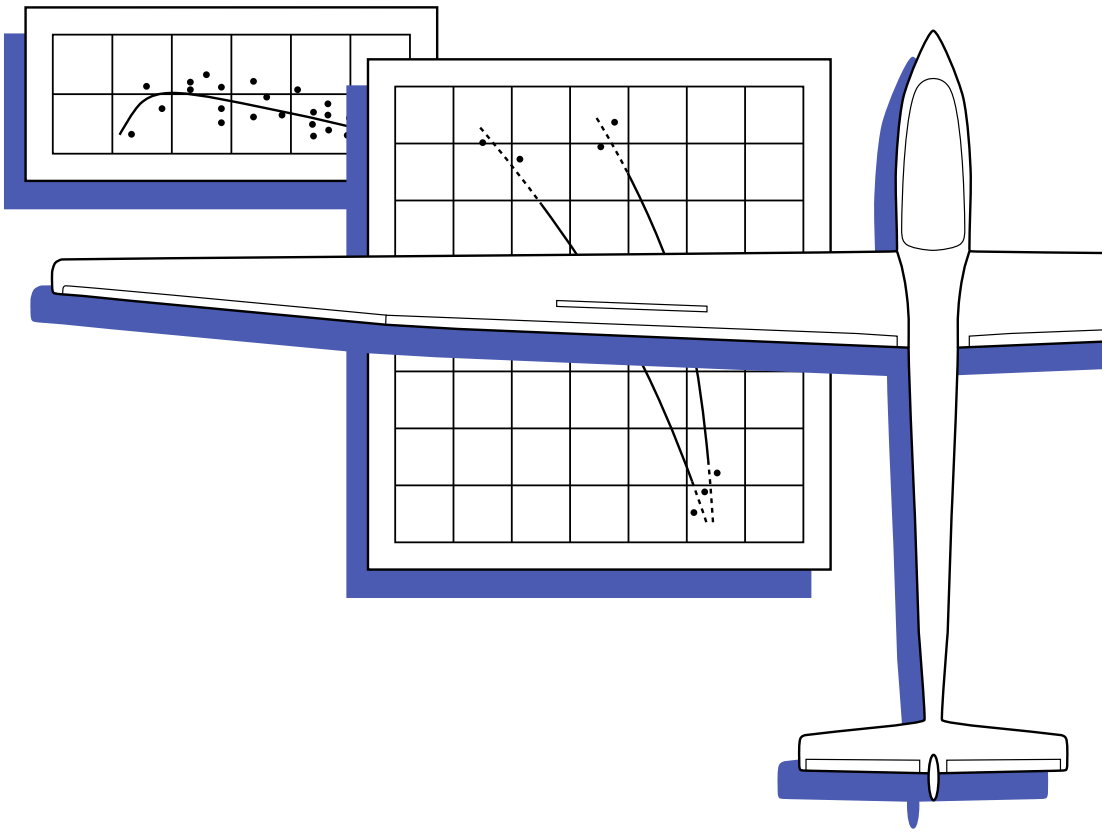

- **Lee Waves without Mountains**

Organisation Scientifique et Technique Internationale du Vol à Voile (OSTIV)
International Scientific and Technical Organization for Soaring
www.ostiv.org

# Technical Soaring

The Scientific, Technical and Operational Journal of
the Organisation Scientifique et Technique Internationale du Vol à Voile
(International Scientific and Technical Organization for Soaring)

**Volume 47, Number 3** **July — September 2023**






ISSN 0744-8996

*Technical Soaring* (*TS*) documents recent advances in the science, technology and operations of motorless aviation.
*TS* is published quarterly by the Organisation Scientifique et Technique Internationale du Vol à Voile (International Scientific and Technical Organization for Soaring, OSTIV), c/o TU Braunschweig, Institute of Fluid Mechanics, Hermann-Blenk Str. 37, D-38108 Braunschweig, Germany. E-mail: `president@ostiv.org`; URL: `www.ostiv.org`.
Subscription is restricted to OSTIV members but material can be submitted by anyone. Annual dues are €25 for Individual/Local Club Membership; €80 for Scientific/Technical Organization/Library Membership and €250 for Active Members (National Aero Club Members of FAI). Students under 25 years of age may join free of charge.
Submitted research papers will be peer-reviewed. Guidelines for preparation and submission of manuscripts can be found in this issue and on the OSTIV website in the 'editor' section.
*TS* is online (full-color) at `journals.sfu.ca/ts/`. Back issues, from Vol. 1, No. 1 to the current issue are online. OSTIV members have complete access to *TS* online; non-members may access titles and abstracts. Members should contact the webmaster, `ts-support@ostiv.org`, for access.
The name *Technical Soaring* and its cover layout are fully rights-protected and belong to the Soaring Society of America; they are used by permission.

## Preparation of Manuscripts for *Technical Soaring*

*Technical Soaring* (*TS*) documents recent advances in the science, technology and operations of motorless aviation. *TS* welcomes original contributions from all sources.

**General Requirements** Manuscripts must be unclassified and cleared for public release. The work must not infringe on copyrights, and must not have been published or be under consideration for publication elsewhere. Authors must sign and submit a copyright form at time of submission. The form is available at `www.ostiv.org`.

**Language** All manuscripts submitted to *TS* must be in English. Submissions requiring extensive editing may be returned to author for proofreading and correction prior to review.

**Layout** Submit manuscripts in single-column, double spaced layout with all figures and tables at end, one per page.

**Electronic submissions** are preferred. Most data file formats are acceptable, with PDF preferred. Submit one file containing the complete paper including all figures, tables, and captions. Paper submissions will also be accepted — contact the Editor-in-Chief (EIC) for submission details.

**Length** There is no fixed length limit. At the discretion of the EIC, manuscripts may be returned to the author for reduction in length.

**Structure** Organize papers as needed in sections, subsections, and subsubsections.

**Title** A title block is required with author name(s), affiliation(s), location, and contact info (email address preferred).

**Abstract** All papers require a summary-type abstract consisting of a single, self-contained paragraph. Suggest 100 to 150 words. Acronyms may be introduced in the abstract, but do not cite references, figures, tables, or footnotes.

**Nomenclature** If the paper uses more than a few symbols, list and define them in a separate table. Otherwise, explain them in the text where first used. Define acronyms in the text following first use.

**Introduction** An Introduction is required that states the purpose of the work and its significance with respect to prior literature, and allows the paper to be understood without undue reference to other sources.

**Conclusions** The Conclusions section should review the main points of the paper. Do not simply replicate the abstract. Do not introduce new material or cite references, figures, or tables in the Conclusions section.

**Acknowledgments** Inclusion of support and/or sponsorship acknowledgments is strongly encouraged.

**Citations** Cite with bibliographic reference numbers in brackets (e.g. "[7]"). Do not cite Internet URLs unless the website itself is the subject of discussion.

**References** All references listed in the References section must be cited in the text. List references in order of first citation in the text. Any format is acceptable as long as all citation data are provided. At a minimum, all types of entries require title, year and manner of publication. Provide full names of all authors. Do not list Internet URLs as sources. However, where possible, include an Internet address to the source of the reference.

**Captions** All figures and tables require captions. Do not use the caption to explain line styles and symbols — use a legend instead.

**Color** Color graphics are acceptable. Avoid using color to distinguish data sets in figures — instead, use line styles, symbol shapes and fill patterns.

**Footnotes** Use footnotes sparingly. Do not footnote to cite literature.

**Numbering** All figures, tables, footnotes and references must be referenced in the text and are numbered sequentially in order of first reference. Equations are numbered only if they are referenced by number in the text. Number every page.

**How to submit** Email all electronic material to the EIC at `ts-editor@ostiv.org`.

**Peer Review** Manuscripts will be peer-reviewed before being accepted for publication. Authors may choose between two options: A full peer review with two independent and anonymous reviewers. In this case authors are welcome to suggest names of reviewers. The second option is the *TS* Fast Track Scheme, with the manuscript being reviewed by the EIC or an Associate Editor. With the publication of an article it will be documented in a footnote on the first page of the article which option was chosen by the author. The EIC or the assigned Associate Editor may be contacted by the author at any time for updates on the status of their review.

**Charges** *Technical Soaring* does not require a publication page-charge.

## From the Editor

### Publication Date

This issue is the third of Volume 47 of *TS*, corresponding to July-September 2023. For the record, the issue was published in September 2024.

### About this issue

In this issue of *Technical Soaring*, Julian West's article "Lee Waves without Mountains" explores an unusual meteorological event over Germany, where lee waves were created not by mountains but by nocturnal land breezes and diurnal sea breezes. The study details the atmospheric dynamics behind the formation of these cloud streets and their propagation over vast distances. West's findings not only deepen our understanding of non-topographic wave formations but also highlight unique soaring opportunities for glider pilots.

Very Respectfully,

Kurt Sermeus
Editor-in-Chief, *Technical Soaring*
ts-editor@ostiv.org

# Lee Waves without Mountains - Extensive wave induced cloud streets over Germany on 14th April 2015

Julian West
westjulian1@gmail.com
*Freising, Germany*

## Abstract

**In the afternoon of 14th April 2015 a series of cumuliform wave cloud streets were observed over Haag an der Amper, Germany. These cloud streets were up to 300 km long with an alignment of 80/260 degrees, and extended for 400 km up/down wind. Analysis of radiosonde data from the region revealed several layers of differing stability, with two significant inversions that enabled the downwind propagation of these cloud streets. This study also explores the atmospheric conditions, typically observed along the North Sea coasts, which initiated the formation of these extensive lee waves. The results indicate that they were created by a nocturnal offshore land breeze, which initiated these waves and determined their alignment and subsequent propagation downwind. Some hours later another set of wave cloud streets, having a slightly shorter wavelength, were created by a diurnal onshore sea breeze. The potential for soaring flights using these unusual waves is also discussed.**

## Nomenclature

| | |
|---|---|
| $g$ | gravitational constant, 9.81 m/s$^2$ |
| $h$ | height in m |
| $T$ | temperature, in Kelvin |
| $U$ | horizontal wind speed, in m/s |
| $\ell$ | Scorer parameter, in m$^{-1}$ |
| $\beta$ | parameter |
| $\lambda$ | wave length, in m |
| $\theta$ | potential temperature, in K |

## Introduction

In the afternoon of 14th April 2015, between 1400 and 1500 GMT (4 to 5 pm), a spectacular set of cumuliform wave bars with cloud (Foehn) fingers, Fig. 1, was observed above Haag an der Amper, which is located 40 km NNW of Munich. They stretched as far as the eye could see in all directions and appeared to be stationary. The surface wind was a light westerly with a northerly component. One of a series of satellite pictures for this period reveals an extensive area of uniform cloud streets with an 80/260 degree alignment covering much of Germany from north of Erfurt to south of Munich, a distance of 400 km. The longest cloud street ran for 300 km from north of Stuttgart to east of Pilzen in the Czech Republic. The forecast surface chart for 12 GMT showed Germany covered by an extensive area of front-free high pressure centred over the Black Forest, with a warm front located just to the east of Denmark.

These stationary lee waves were not created by a topographical barrier, such as a mountain ridge, but by a coastal land breeze. A land breeze is a nocturnal offshore gravity current which, in this case, initiated lee waves covering an extensive area downwind. These waves were marked by a series of cumuliform wave cloud streets parallel to the North Sea coasts of Germany and Holland. All heights given here and later in this paper are AMSL, unless otherwise stated.

A series of satellite pictures taken during this period confirmed that the cloud streets were indeed stationary. The wave bars in this area were not aligned perpendicularly to the wind flow but parallel to the coast, and their 11 km spacing corresponded to a wavelength along the wind of 13.4 km, which is

**Fig. 1: The cumiliform wave cloud streets viewed from the ground.**

This article was peer reviewed by two independent, anonymous reviewers.

twice that expected from the general estimate for the lee wavelength given by $\lambda = (0.6 \cdot U – 3) = 6.6$ km, where $U$ is windspeed in m/s.

The Meteosat geostationary satellite picture for 1500 GMT, Fig. 2, reveals an extensive area of uniform cloud streets aligned 80/260 degrees and covering much of Germany from north of Erfurt to south of Munich, a distance of 400 km. The longest cloud street ran from just north of Stuttgart to slightly east of Pilzen in the Czech Republic, a distance of 300 km. The wave cloud lines appeared to be unrelated to the underlying topography and the COSMO vertical wind forecasting model, which takes account of the topography, did not show any up- or downdrafts with alignments corresponding with these cloud lines. Unfortunately, no records of any sailplane flights exploiting the cross-country potential of these cloud streets have been found for this day. The purpose of this research is to determine the origin of these lee waves and to explain their extensive propagation.

## Synoptic Situation

An investigation by Wallington [1] showed that, ahead of a well-marked surface warm front, with a 3-layer model lee waves were likely to be significant in two zones. Ahead of the warm front investigated, lee-waves were calculated and observed to be particularly pronounced at low levels in a zone between about 240 and 400 km ahead of the surface position of the front. Pro-

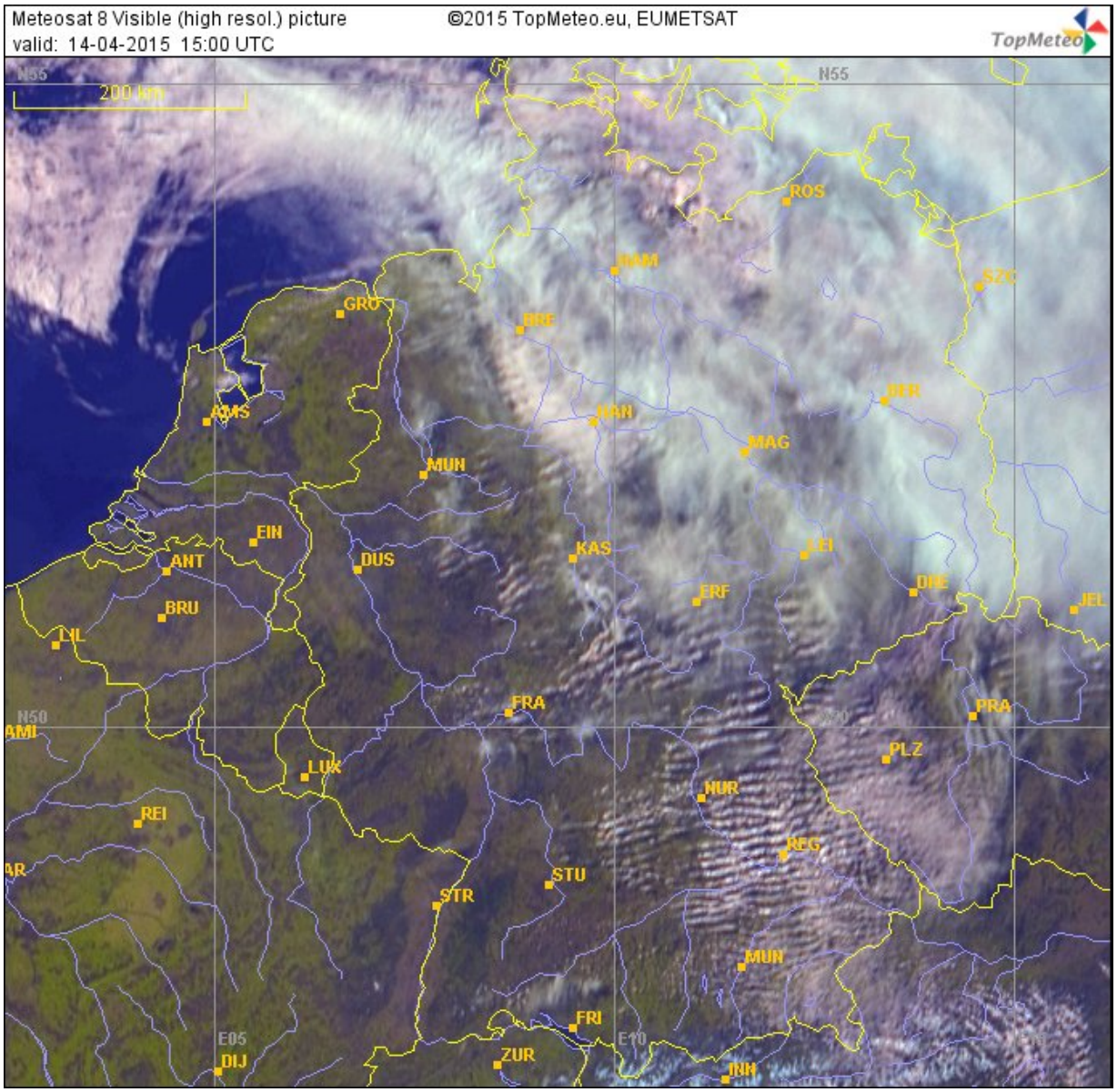


**Fig. 2: Lee wave induced cloud streets at 15:00 GMT on 14.04.2015.**

nounced leewave flow was also possible at both high and low levels at distances between 640 and 960 km ahead of the front. Between these zones short lee waves were possible but with insignificant amplitudes.

The actual surface chart for 06:00 GMT, Fig. 3, shows a surface warm front, progressing across the North Sea towards Poland from the northwest, which would create conditions ahead suitable for lee waves over Poland. The whole area of Germany is covered by an area of high pressure centred on the Black Forest. The same chart for 12 GMT, Fig. 4, shows that Germany remains covered by an area of front-free high pressure centred over the Black Forest, but the warm front is now located just to the east of Denmark. As such, these charts give no indication of the airmass over Germany being in any way suitable for lee waves. However, they are favourable for land breeze formation at the North Sea coast.

The Meteosat picture for 12 GMT, Fig. 5, depicts a similar set of wave bars over eastern Germany, which are aligned with a section of the coast at Rostock. This picture also shows longer wavelength waves over Poland aligned with the Baltic Sea coast, with shorter wavelengths beneath them, as described by Wallington [1] and discussed in the Appendix.

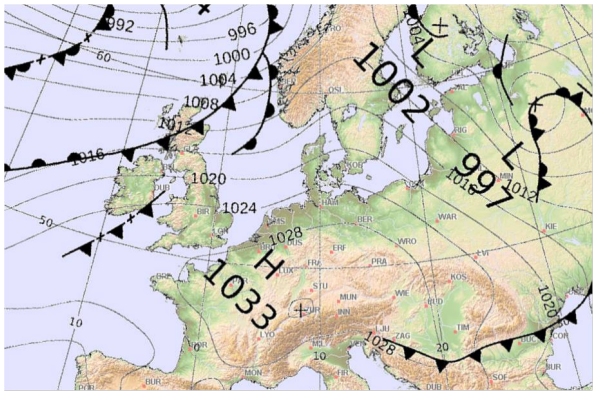


**Fig. 3: Actual surface chart for 06 GMT on 14.04.2015.**

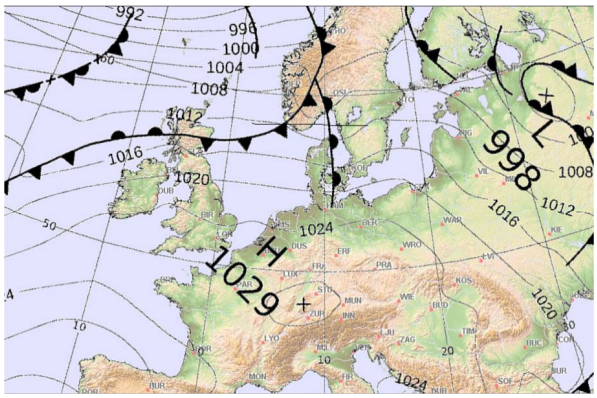


**Fig. 4: Actual surface chart for 12 GMT on 14.04.2015.**

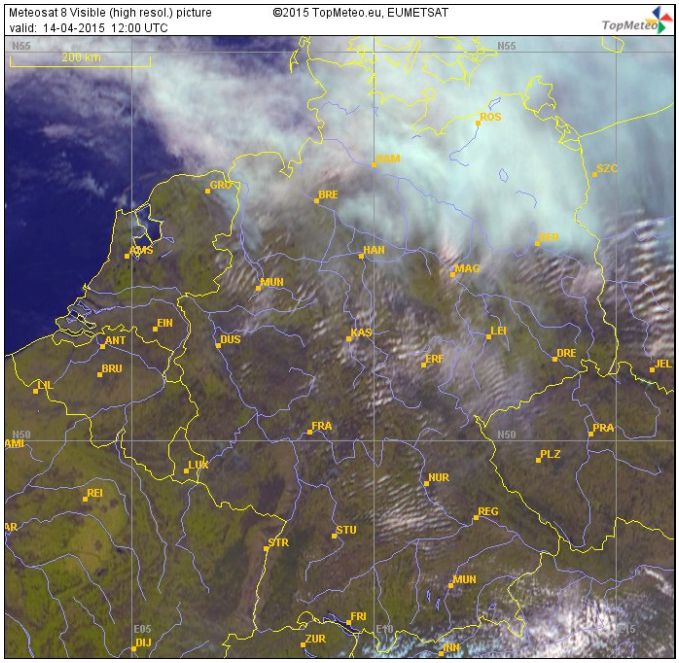


**Fig. 5: Lee wave induced cloud streets at 12:00 GMT on 14.04.2015.**

## Data Analysis

Radiosonde soundings from the affected areas of Germany and the Czech Republic have been examined and two of them are described in more detail below. They are all rather similar, typically comprising a bottom layer with extremely low stability (9.5 C/km) capped at around 2,000 m by very thin inversion. Above that is a layer with moderate stability (6 C/km) capped at about 3,500 m by another very thin inversion, above which there is a very deep layer with low stability (8 C/km). Radiosonde data are affected by vertical air motion, consequently the temperature profiles from balloon ascents will be distorted by passage through waves. Relative to that of the undisturbed flow, in an ascending current the stability will be reduced and in a descending current it will be increased, Scorer [2]. The most relevant data were the 12 GMT sounding for Kuemmersbruck (Amberg), which was geographically closest to and just two hours upwind of the lee wave clouds of Fig. 1; and the 00 GMT sounding for Norderney, which is about 12.5 hours upwind. The 00 GMT sounding for Norderney shows an average 2 m/s offshore wind component up to 750 m, and a 7.6 m/s onshore wind component from 1,700 m.

The 12:00 GMT Kuemmersbruck sounding, Table 1, displays an initially almost dry adiabatic environmental lapse rate (ELR) up to 1,250 m, and then an almost wet adiabatic ELR up to 1,900 m. This is followed by two thin inversions, above which is a 300 m thick isothermal layer. Above this a 1,300 m deep moderately stable layer is topped by third inversion at 2,300 m, with a 300 m deep isothermal layer above that. At 3,800 m there was a fourth thin inversion topped by a third 300 m thick isothermal layer. From 4,200 m upwards there was a 9,000 m thick layer of

low stability

At the surface there was an 4 m/s westerly wind which gradually increased with height veering to a northwesterly at 2,300 m, above which the speed (15 +/- 1.5 m/s) remained almost constant up to 6,400 m. Above that the windspeed steadily increased to 27 m/s at 10,800 m. The wind direction veered favourably from 313 to 350 deg, up to 7,800 m .

Below 1,250 m the static stability was almost neutral. Above that the potential temperature $\theta$ increased upwards, indicating that the static stability $g \cdot \beta$, where $\beta = (1/\theta) \cdot (d\theta/dz)$, and the Scorer parameter $\ell = \sqrt{g \cdot \beta / U^2}$ were positive, as is to be expected for lee waves. The ELR in the convection layer suggests blue thermals up to 1,500 m (1,100 m AGL). With a measured wavelength of 13.4 km along the wind, the maximum vertical wind component would be 1.5 m/s for a wave amplitude of 500 m.

## Potential Cloud Levels

From the dewpoint depression (dpd) at 1,690 m, 3.7 °C, the lowest possible cloudbase is at 2,065 m, with tops at the 2,300 m inversion. This implies a minimum wave amplitude of 375 m (= dpd x 101.4). At 1690 m the wave bar crosswind component is 6 m/s, not too far below Nicholls' [3] minimum of 7 m/s at the crest of a low ridge.

At 1,930 m the dew point depression is 4.1 °C, which indicates a second cloud base about 415 m higher at 2,345 m with cloud tops at the 2,650 m second inversion. This would require a minmum wave amplitude of 415 m at this level.

The dew point depression at 2,900 m is 4.7 °C, giving a potential third cloudbase at 3,375 m, with tops at the 3,800 m third inversion. This implies a minmum wave amplitude of 475 m at this level. The slope of the ELR is 6 °C/km, and is absolutely stable above 2,400 m, so any clouds would have a smooth, possibly lenticular, form.

The maximum relative humidity was 90% at 3,850 m, with a potential cloud base of 3,980 m, for a minimum wave ampitude of 130 m. As this very high humidity was within a fourth 50 m inversion, any clouds would be thin and have a smooth form. The wavebar crosswind component decreased upwards from 3,900 to 5,900 m, which would reduce the wave amplitude upwards. Although there are no clouds visible at this level in Fig. 1, they are featured in Fig. 10 below.

## Linear Lee Wave Theory

In suitable conditions lee waves can occur at a discontinuity of stability. For the wave equation to have one or more real solutions, so that an infinite train of trapped lee waves can develop, the Scorer parameter must decrease upwards. If this parameter increases with height, although there can be no real solution, there may still be a complex one which would imply a wave train that decayed exponentially downwind. The mathematical analysis of a 2-layer atmosphere with a stability discontinuity, Scorer [2], gives a useful insight into the general nature of wave flow, which could also be applicable to more complex models.

The equation for the 2-layer model with lower (i) and upper (s) layers, Scorer [4], is:

$$u_i – u_s \cdot i \cdot tan(u_i \cdot h_i) = 0, \tag{1}$$

where $u = \sqrt{k^2 - \ell^2}$, $h$ is the depth, $\ell^2 = g \cdot \beta / U^2 - (1/U) \cdot d^2U/dz^2$, $k = 2 \cdot \pi / \lambda$, $\beta = (1/\theta) \cdot d\theta/dz$, $\lambda$ is the wavelength, and $\theta$ the potential temperature.

For real solutions $\ell_i > \ell_s$, and $i = \sqrt{-1}$ in Eq. 1 can be eliminated by the relations $i^2 = -1$ and $i \cdot tan(i \cdot x) = -tanh(x)$. For trapped lee waves,

$$\ell_i^2 > k^2 > \ell_s^2 \tag{2}$$

From the data $\ell_i^2$ is 0.93 km$^{-2}$ on average, implying a wavelength of 6.5 km; and $\ell_s^2$ is 0.17 km$^{-2}$ on average, implying a wavelength of 15 km. For the observed 13.4 km along the wind wavelength $k^2$ = 0.22 km$^{-2}$, thereby fulfilling the condition of Eq. 2 above.

With the 2-layer model trapped lee waves have their maximum amplitude somewhat below the level of the discontinuity concerned. It varies sinusoidally downwards, and decreases exponentially upwards, away from this level. The largest amplitudes occur when the half-height ridge width equals $\lambda/\pi$. In the majority of cases when wave actually occurs in the atmosphere this model has no solution.

Better results are obtained from the more realistic 3-layer model, whereby a convecton layer (c) is inserted below those of the 2-layer model. Wallington [1] assumes that the lowest layer is rendered adiabatic ($\ell_c = 0$) by convective mixing, which is almost the case here. He also suggests that shallower convection layers give greater wave amplitudes. The general equation for a multi-layer model, together with graphical solutions for the wavelength(s) of models with up to five layers, is given in West [5]. An example of the 5-layer model exhibits two real solutions with $\lambda$ = 7.5 km and 15 km.

According to an analysis of the 3-layer model by Zang, Zhang and Huang [6], the lee wavelength increases with a decrease in the thickness of the lower and middle layers, being more sensitive to changes in the middle layer. The wavelength also increases with a decrease in the value of the Scorer parameter in every layer, being most sensitive to its value in the upper layer. As the value of the Scorer parameter $\ell_s$ of the upper layer is relatively low and steadily increases with height ($U$ = 14 to 27 m/s, and $dT/dz$ = 8°C/km), any lee waves are trapped and have a long wavelength. The three layer model gives ony a single solution for the lee wavelength.

In this particular case, the radiosonde soundings suggest that a 5-layer model with two inversions would be more appropriate than a 3-layer model. A 5-layer model provides an additional longer wavelength solution with a smaller amplitude, West [5], which might be a better match to the nose profile of a gravity current. Even a relatively small proportion of a double wavelength would suppress cloud formation at alternate wave crests, and

this could explain the observed wavelength of 13.4 km rather than the expected 6.6 km referred to earlier.

The possibility that these cloud streets are shear waves can be ruled out by the almost complete lack of significant horizontal and vertical shear in the wind profile. This provides further confirmation that the cloud streets observed on 14.04.2015 were caused by lee waves. The constant ($U_i$), or steadily increasing ($U_s$), wind speeds also imply that the wind profile correction term $(-(1/U).d^2U/dz^2)$ in the Scorer parameters ($\ell_i^2$ and $\ell_s^2$) can be neglected.

## Convective Lee Wave Clouds

The wave clouds in Fig. 1 are not lenticulars, which are smooth clouds with a lens shaped outline, but are altocumulus wave bars. They are officially known as as roll clouds, and have derived this name from the illusion of rotation caused by shear between its base and top, as explained by Scorer [4]. Such wave clouds are cumuliform due to the conditional stability of the layer in which they occur, and do not indicate the presence of either rotors or thermals. Smooth wave clouds, which are not always lenticulars, only occur at a level where the atmosphere is absolutely stable, [7].

Saturated air, unlike unsaturated air, has a lapse rate that is temperature dependent because it holds more moisture at higher than lower temperatures. On a Stüve chart the saturated adiabatic lapse rate (SALR) lines are curves that are asymptotic to the dry adiabatic lapse rate (DALR) lines, whereby the SALR slope approaches that of the DALR but never meets it. An SALR isocline (equal slope) for the stable ELR lapse rate of the Standard Atmosphere (6.5 °C/km) is shown in Fig. 6, together with three ELR lines this lapse rate. Below the level at which the ELR intercepts an SALR isocline with the same lapse rate saturated air is unstable (conditional stablility), and so wave clouds forming there will be convective. Above this level saturated air is stable (absolute stability) and wave clouds forming there will have a smooth stable form. The transition level between conditional and absolute stability occurs at the altitude of the intersection between an ELR and the SALR isocline with the same lapse rate. This altitude depends mainly on the temperature at which a downwardly extended ELR intersects the MSL base line. As can be seen from Fig. 6, the transition altitude for a 6.5 °C ELR line is much higher in summer than in winter. This leads to a marked seasonal variation of the vertical distribution of cumuliform and lenticular wave clouds. For the Kuemmersbruck sounding stable wave clouds, such as lenticulars, can only form above 3,500 m.

According to Hauf and Clark [8], convective clouds do not form a significant barrier to airflow unless they contain thermals. Consequently, only if there were thermals within the convective wave clouds would there be a barrier effect.

## Centrifugal Waves

Where the motion is sufficiently curved and the velocity gradients large, centrifugal forces can play a part similar to gravitational forces, Scorer and Wilson [9]. Where a shear layer enters

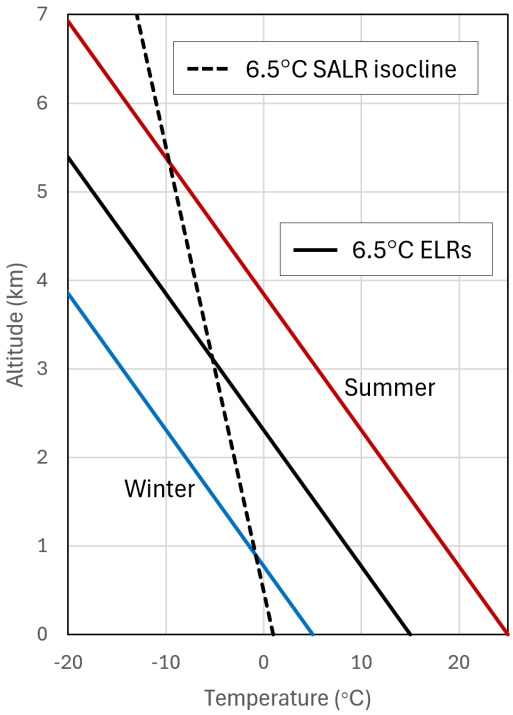


**Fig. 6: Intersection of 6.5 °C ELRs with the 6.5 °C SALR isocline.**

the wave motion the faster moving fluid tends to move to the outside of any curve in the flow. Thus if the faster fluid is on top it will tend to move under the slower moving fluid beneath it in the trough of a wave. As soon as the air enters the next wave crest a formerly unstable layer becomes very stable, so that longitudinal corrugations spread laterally across the cloud as stable waves, ready to grow again in the next trough. In this way they can persist for some distance in an area of waves. They may extend as cloud fingers into the gap between wave bars. Their wavelength is that of the stable layer in which they propagate. This secondary instability only occurs when the curvature and shear together are enough to overcome the static stability.

Figure 7, from Scorer [10], shows the corrugations growing as the air proceeds through a wave trough. The fingers extending from the clouds in the photograph of Fig. 1 indicate the presence of centrifugal waves. Although here the vertical shear is extremely low, it is still sufficient to overcome the very low static stability in the lowermost layer. They are often called "Foehn" fingers, because they commonly feature in the wave clouds of the warm alpine wind having that name. However, here the wind is a cold northerly rather than a warm southerly.

The stable layer here is actually two thin 300 m thick isothermal layers separated by a thicker 1,300 m less stable layer. Each stable layer has a less stable layer above and below it, giving the possibility of centrifugal waves at several levels. The isothermal layer Scorer parameters, $\ell_i^2$ = 1.38 and 1.33 km$^{-2}$, are almost equal with 5.36 & 5.46 km wavelengths. For the thicker less

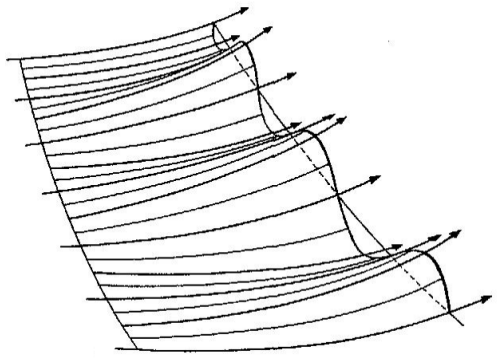

**Fig. 7: Longitudinal corrugations in a wave trough. Adapted from Scorer [10], under fair use.**

stable layer $\ell_i^2$ = 0.7 km$^{-2}$ and the wavelength is 7.67 km. This could account for there being centrifugal waves with two distinct wavelengths of about 4 and 6 km, which can be seen on the satellite picture of Fig. 2.

## Land and Sea Breeze Gravity Currents

The area of lee waves over southern Germany, shown in Fig. 2, appear to originate from the north coasts of Holland and Germany to the west of Denmark. From their position in the wave pattern and their 80/260 degree orientation, the cloud streets of Fig. 1 above Haag an der Amper correspond well with alignment of the coast adjacent to the East Friesian Islands. This suggests that the lee waves could be the result of a coastal meteorological phenomenon such as a land breeze. The formation of an offshore land breeze overnight is favoured by a moderate wind aligned along the coast. The effect of a land breeze is to deflect the wind at low levels offshore at a slight acute angle to the coast.

Overnight the land air cools more rapidly than that over the sea resulting in a density discontinuity of 0.33% per 1°Cof temperature difference. The denser land air subsides creating a gravity (density) current flowing slowly offshore beneath the sea air during the night. As the denser land air meets the warmer sea air the leading edge forms a nose as the land air rolls back on itself, as shown in Fig. 8 after Simpson [11]. This nose is about twice the height of the main circulation, and creates a cross-wind ridge of denser cold air that triggers lee waves in the warmer sea airflow above, Fig. 8. The humidity associated with the sea air aloft flowing southwards then facilitates the formation of a series of convective cloud streets aligned along the wave crests.

The variation of the onshore and offshore wind components with height at Norderney is shown in Table 2. This indicates that there would have been an offshore land breeze extending up to 750 m. Table 2 also shows that the height of the crosswind barrier necessary for the formation of lee waves was at least 1700 m, where the windspeed was 12 m/s at 300 deg. The onshore component was 7.6 m/s, which is above the minimum of 7 m/s at the crest of a low ridge as stated by Nicholls [3]. Above this level the onshore wind component increased with height up to 2,700 m. The sounding exhibits two thin stable layers, at 1,550 and 2,750 m, with a layer of lesser stability between them. The potential temperature $\theta$ increased upwards indicating that the static stability $g \cdot \beta$ and the Scorer parameter $\ell$ were positive, as expected for lee waves.

The structure of a gravity current is shown in Fig. 8 above. Note the relative flow of shallow surface cold air (blue arrows) towards the leading edge, and strong ascent (red arrows) ahead of the current. Circulation at the nose is shown with entrainment of pre-frontal air (green arrows) which raises its height substantially.

The nose of a gravity current can have irregularities in the form of clefts, as shown in Fig. 8, which for an onshore sea breeze are caused by ground features. A land breeze over the sea would not normally be expected to have these clefts, but in this case the gravity current has crossed the East Friesian Islands. The land breeze blows offshore at a slight acute angle with the coastline, and its major component is directed eastwards along the coast. The series of satellite photographs, which were taken between 1400 and 1500 GMT, display cloud features that are moving eastward at about 19 km/h along the wave bars, which is also the average speed that the gravity current travelled along the coast. The series also show the wave bars moving slowly in a southsoutheasterly direction, which could be due the wind veering slightly thereby marginally increasing the spacing of the wave bars.

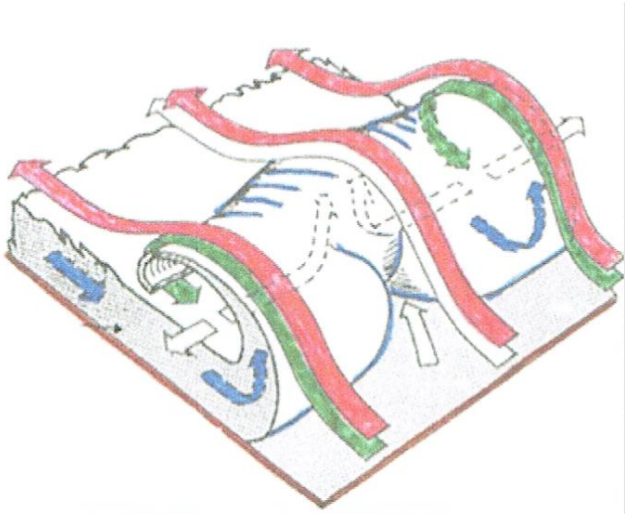

**Fig. 8: Formation of a nose on a land or sea breeze gravity current.**

## Timing of the Event

The diurnal variation of sea and land breezes, after Pokhrel & Lee [12], is depicted in Fig. 9, which indicates a maximum offshore speed at 5:30 am of 1 m/s at 10 m above the surface, compared to an offshore wind of 2.4 m/s at GMT midnight here. However, the velocity of the nose itself might be less than this. The hatched areas show time periods corresponding to the two

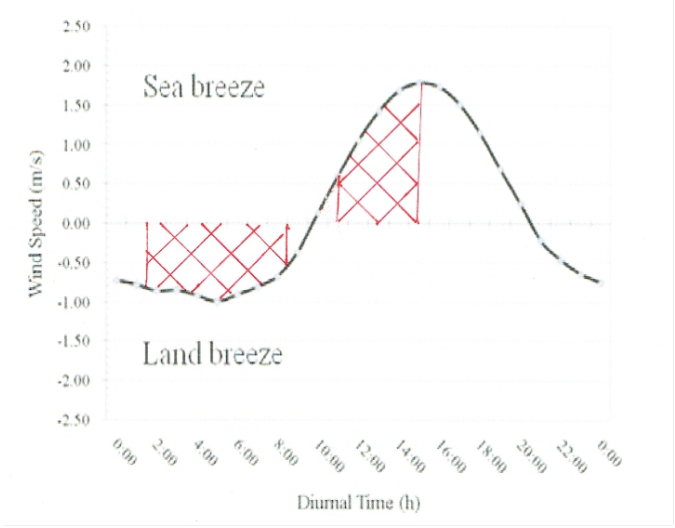


**Fig. 9: Diurnal variations of the lee waves and of land & sea breezes.**

separate sets of wave bars shown on the 15:00 GMT picture of Fig. 2.

At Haag an der Amper in Bavaria, with a steady wind speed of 56 km/h above the convection layer, the event observed from 14 to 15 GMT by the author would have happened at the coast some 12.5 hours earlier. The 7 hour duration of this event, from about 1 am to 8 am local time at the coast, corresponds to the time when there could well have been a significant land breeze offshore gravity current from the north coasts of Germany and Holland, which are adjacent to the line of East Friesian Islands. If a land breeze can initiate lee waves, then a significantly stronger sea breeze onshore gravity current could well do the same. While the satellite picture for 12:00 GMT, Fig. 5, does not show any waves close to the coast, that for 15:00 GMT, Fig. 2, shows another set of lee waves that are much nearer to the coast. There seems to be a 2.5 hour gap, between wave bars from the sea and land breezes between Hannover to Erfurt, as would be expected from Fig. 9, with another set of lee waves of 4 hours duration, initiated by the coast from 10:30 am to 2:30 pm local time. These could be created by the nose of a sea breeze onshore gravity current. As the noses of the land and sea breezes move in opposite directions, the "doppler effect" will increase the wavelength of the first set of waves and decrease the wavelength of the second set. This appears to be the case here, as the wavelength of the last few waves of the first set is one sixth greater than that of the first few waves of the second set. This suggests that the sum of the velocity magnitudes for the land and sea breeze noses is 1.7 m/s, which is reasonably consistent with Fig. 9.

## Effects of Angular Shear

Although these waves were intiated during the night, they do not appear on satellite photographs until midday GMT. The 00Z Norderney sounding for 14.04.2015, Table 2, had an isothermal layer from 1,500 to 1,700 metres making it suitable for lee waves iniated by a similar height ridge. However, the lowest dewpoint depression is 7°C at 2,500 m, which would require wave amplitudes at this level of over 700 for cloud to form. As satellite pictures taken during the morning do not show wave clouds, any lee waves must have had a lesser amplitude at these levels.

Over long distances angular shear alters the humidity profile, which affects the condensation level(s) and the wave amplitude(s) required for clouds to form. The 12Z Kuemmersbruck sounding, Table 1, displays a dewpoint depression of only 2.6°Cat 2,300 m, which would result in cloud formation if the wave amplitude exceeded 260 m. Allowing for an angular shear of 40 degrees between 1,700 and 4,000 m, the Kuemmersbruck airmass at the levels of these waves comes from an 80 km long section of the North Sea coast.

The angular shear also changed the temperature profile, rendering it more favourable for waves, and this could increase the wave ampliude and affect its variation with height. Such changes can result in wave clouds first appearing in areas well away from where they were initiated, and any resulting amplification of these waves could enhance their downwind propagation.

## Altocumulus Lenticularis

Later on smooth stable clouds were to be seen near Ingolstadt, 60 km further northwest, as shown in Fig. 10. These shallow smooth clouds were at 4,000 m, where the air was absolutely stable, and there were not any convective wave clouds beneath them. The wave amplitude at this level would have been 130 m, the minimum for cloud, plus the cloud depth. This implies a vertical wind component of 0.5 m/s, which corresponds with the authors experience that the best climb rates in wave are often not found in front of spectacular lenticulars such as these. Where the air is too dry for continuous wave bars then individual wave clouds, such as altocumulus lenticularis, may form instead. Some indication of short wavelength centrifugal waves can also be seen in the photograph of Fig. 10.

**Fig. 10: Lenticular clouds during the early evening of 14.04.2015.**

## Soaring Potential

The meteorological climb rate at the level of the cumuliform wave clouds is 1.5 m/s, at 2,300 and 2,900 m, but at that of the higher lenticular clouds is only 1 m/s at 3,800 m. In order to connect with these either a motorglider, or a tow to about 1,500 m AGL, would have been necessary. At 2,300 and 2,900 m the 15.4 m/s (56 km/h) wind speed would result in head and tail winds along the wave bars of 33.4 and 22.6 km/h, respectively. In Germany the maximum flight altitude is limited to 3,000 m by airspace rules, so this would not have been a problem. The air temperature at flight levels varied between -1.5 to -4°C, so it would not have been excessively cold, but not ideal for carrying water ballast. As these waves were not influenced by the topography, the cloud alignment would not have been affected by wave interference effects, and the optimum route in front of the clouds would have been very easy to follow. As the wave amplitude was small relative to the wavelength, rotor or other clear air turbulence was unlikely.

For an Antares 20E motorglider, at 600 kg maximum take-off weight a sink rate of 1.5 m/s occurs at an airspeed of 195 km/h, which from Table 1 would give head/tail winds of 33 and 23 km/h at 2,300 and 2,900 m, respectively. The ground speeds would be 223 km/h or 211 km/h to the east and 156 km/h or 166 km/h to the west. At these speeds a 750 km three turning point task, whether flown at 2,300 or 2,900 m, would theoretically have taken less than 4 hours. As the waves were already visible at 12:00 GMT (2 pm local time), and probably remained visible until 16:00 GMT (6 pm local time), possibly only as smooth wave bars at 4,000 m, as shown in Fig.10, such a flight is not unrealistic.

## Conclusions

1. This particular event demonstrates that lee waves can propagate downwind over land for a distance of 800 km, all the way from the North Sea coast to the Alps. The wave bars extended across the prevailing wind at their level, for about 300 km from Stuttgart to Pilzen. They were aligned with the North Sea coast, without there being any significant upwiind topographical barrier such as that usually provided by a mountain ridge.

2. The perturbation responsible for the lee waves at Haag an der Amper was a nocturnal offshore land breeze along the North Sea coasts of Holland and Germany (circa 300 km). A land breeze is a low level gravity current that flows offshore at an acute angle to the coast. The nose of this gravity current formed a long uniform pseudo ridge that initiated a 300 km wide by 400 km long area of lee waves during a 7 hour period.

3. The onshore gravity current of a sea breeze, which is somewhat stronger than that of a land breeze, can also initiate lee waves, such as those in Fig. 2 between the coast and Hannover. Because a land breeze is moving onshore it is less suitable for lee wave formation than a land breeze moving offshore against the prevailing wind.

4. Angular shear is not necessarily detrimental to lee wave formation, provided the wind direction at altitude becomes nearer to the ridge perpendicular. There is no specific angular limit for the wind direction away from the perpendicular, the strength of the cross wind component over a ridge being a better criterion for lee waves. An adverse angle to a ridge perpendicular has the effect of broadening it, which can provide a better match to the lee wavelength.

5. Over long distances angular shear can significantly alter the humidity profile, which affects the condensation level(s) and the wave amplitude(s) required for clouds to form. It will also change the temperature profile, in this case rendering it even more favourable for waves. This could also affect the variation of the wave amplitude with height. Such changes might result in wave clouds first appearing in areas well away from where they were initiated, and could also amplify them, thereby enhancing their propagation downwind.

6. As these cloud streets were visible for many hours, they would have been suitable for out and return tasks. Soaring flights exceeding 750 km would have been possible by flying mostly along the upwind sides of the wave bars in both easterly and westerley directions. Either a motorglider, or an aerotow to 1,500 m AGL, would have been necessary to access the lines of lift.

## References


[1] C. E. Wallington. Lee waves ahead of a warm front. *Quarterly Journal of the Royal Meteorological Society*, 81:251–257, 1955. doi:10.1002/qj.49708134811.

[2] R. S. Scorer. *Environmental Aerodynamics*, chapter 5. Ellis Horwood, 1978.

[3] J. M. Nicholls. *The Airflow over Mountains research, 1958–1972*. Number 127 in WMO Tech. Note. 1973. URL: https://library.wmo.int/idurl/4/30048.

[4] R. S. Scorer. Theory of waves in the lee of mountains. *Quarterly Journal of the Royal Meteorological Society*, 75:41–56, 1949. doi:10.1002/qj.49707532308.

[5] J. M. West. Lee wave interference patterns. *Technical Soaring*, 20(2):54–63, 1996. URL: https://journals.sfu.ca/ts/index.php/ts/article/view/538.

[6] Z. Zang, M. Zhang, and H. Huang. Influence of the Scorer parameter profile on the wavelength of trapped lee waves. *Journal of Hydrodynamics, Ser. B*, 19(2):165–172, April 2007. doi:10.1016/S1001-6058(07)60044-4.

[7] J. M. West. Wellen- oder Rotorwolken? Misdeutete Zeichen am Himmel. *Aerokurier*. Feb. 1991, pp. 124–125.

[8] T. Hauf and T. Clark. Convective waves and cumulus growth. *Technical Soaring*, 12(4), 1988. URL: https://journals.sfu.ca/ts/index.php/ts/article/view/805.

[9] R. S. Scorer and S. A. K. Wilson. Secondary instability in steady gravity waves. *Quarterly Journal of the Royal Meteorological Society*, 89:532, 1963. doi:10.1002/qj.49708938208.

[10] R. S. Scorer. *Clouds of the World: A Complete Color Encyclopedia*, chapter 6, page 91. David & Charles, 1972.

[11] J. E. Simpson. *Sea Breeze and Local Winds*. Cambridge University Press, 1994.

[12] R. Pokhrel and H. Lee. Estimation of the effective zone of sea/land breeze in a coastal area. *Atmospheric Pollution Research*, 2:106–115, 2011. doi:10.5094/APR.2011.013.

**Table 1: 10771 ETGK Kuemmersbruck Observations at 12Z 14 April 2015**

| Height metres | Temp. deg. C | Dewpoint deg. C | Dewpoint deprn. C | Relative Hum. % | Theta deg. K | Wind knots | Wind dir. deg. | Angle off perp. deg. | Wind m/s | Crosswind comp. m/s |
|---|---|---|---|---|---|---|---|---|---|---|
| 418 | 13.00 | -2.00 | 15.00 | 35 | 287.9 | 8 | 280 | 70 | 4.12 | 1.41 |
| 495 | 10.80 | -6.20 | 17.00 | 30 | 286.4 | 8 | 279 | 71 | 4.12 | 1.34 |
| 889 | 7.00 | -6.00 | 13.00 | 39 | 286.5 | 12 | 275 | 75 | 6.17 | 1.60 |
| 996 | 6.00 | -6.20 | 12.20 | 41 | 286.5 | 10 | 265 | 85 | 5.14 | 0.45 |
| 1259 | 3.40 | -6.60 | 10.00 | 48 | 286.5 | 16 | 274 | 76 | 8.23 | 1.99 |
| 1576 | 1.80 | -2.80 | 4.60 | 72 | 288.0 | 23 | 285 | 65 | 11.83 | 5.00 |
| 1691 | 1.20 | -2.50 | 3.70 | 76 | 288.6 | 24 | 289 | 61 | 12.35 | 5.99 |
| 1904 | -0.30 | -8.30 | 8.00 | 55 | 289.2 | 27 | 298 | 52 | 13.89 | 8.55 |
| 1934 | -0.10 | -4.20 | 4.10 | 74 | 289.7 | 27 | 299 | 51 | 13.89 | 8.74 |
| 2295 | -1.90 | -4.50 | 2.60 | 82 | 291.5 | 30 | 313 | 37 | 15.43 | 12.33 |
| 2336 | -1.50 | -15.50 | 14.00 | 36 | 292.4 | 31 | 314 | 36 | 15.95 | 12.90 |
| 2357 | -1.50 | -15.50 | 14.00 | 34 | 292.6 | 31 | 315 | 35 | 15.95 | 13.06 |
| 2378 | -1.50 | -16.50 | 15.00 | 31 | 292.8 | 31 | 315 | 35 | 15.95 | 13.06 |
| 2598 | -1.90 | -18.90 | 17.00 | 26 | 294.7 | 30 | 320 | 30 | 15.43 | 13.37 |
| 2901 | -3.30 | -8.00 | 4.70 | 70 | 296.4 | 30 | 326 | 24 | 15.43 | 14.10 |
| 2978 | -3.70 | -13.70 | 10.00 | 46 | 296.8 | 30 | 327 | 23 | 15.43 | 14.21 |
| 3045 | -4.30 | -10.30 | 6.00 | 63 | 296.9 | 29 | 328 | 22 | 14.92 | 13.83 |
| 3123 | -4.70 | -14.70 | 10.00 | 46 | 297.2 | 29 | 330 | 20 | 14.92 | 14.02 |
| 3259 | -5.50 | -9.80 | 4.30 | 72 | 297.8 | 32 | 326 | 24 | 16.46 | 15.04 |
| 3316 | -5.80 | -13.60 | 7.80 | 54 | 298.1 | 33 | 325 | 25 | 16.98 | 15.39 |
| 3513 | -6.70 | -26.70 | 20.00 | 19 | 299.3 | 32 | 326 | 24 | 16.46 | 15.04 |
| 3655 | -7.50 | -13.50 | 6.00 | 62 | 299.9 | 32 | 328 | 22 | 16.46 | 15.26 |
| 3763 | -8.10 | -15.10 | 7.00 | 57 | 300.4 | 31 | 328 | 22 | 15.95 | 14.79 |
| 3836 | -6.90 | -8.20 | 1.30 | 90 | 302.6 | 31 | 329 | 21 | 15.95 | 14.89 |
| 3885 | -6.70 | -8.30 | 1.60 | 88 | 303.4 | 31 | 329 | 21 | 15.95 | 14.89 |
| 4199 | -7.10 | -11.10 | 4.00 | 73 | 306.4 | 29 | 332 | 18 | 14.92 | 14.19 |
| 4651 | -10.10 | -14.30 | 4.20 | 71 | 308.1 | 27 | 335 | 15 | 13.89 | 13.42 |
| 5720 | -17.30 | -21.90 | 4.60 | 67 | 311.9 | 29 | 335 | 15 | 14.92 | 14.41 |
| 5886 | -18.30 | -23.30 | 5.00 | 65 | 312.6 | 30 | 334 | 16 | 15.43 | 14.84 |
| 6395 | -22.30 | -27.70 | 5.40 | 62 | 313.9 | 31 | 330 | 20 | 15.95 | 14.99 |
| 7350 | -29.90 | -35.90 | 6.00 | 56 | 316.1 | 35 | 345 | 5 | 18.01 | 17.94 |
| 7622 | -32.30 | -36.00 | 3.70 | 70 | 316.4 | 37 | 346 | 4 | 19.03 | 18.99 |
| 8926 | -41.70 | -47.70 | 6.00 | 52 | 329.8 | 46 | 353 | -3 | 23.66 | 23.63 |
| 9055 | -42.90 | -46.30 | 3.40 | 69 | 320.9 | 47 | 354 | -4 | 24.18 | 24.12 |
| 9251 | -44.50 | -52.50 | 8.00 | 40 | 321.3 | 48 | 355 | -5 | 24.69 | 24.60 |

**Table 2: 10113 Norderney Observations at 00Z 14 April 2015**

| Altitude metres | Temp. deg. C | Dewpoint deg. C | Dewpoint depr. C | Relative hum. % | Theta deg. K | Wind knots | Dir. deg. | Angl. off perp. deg | Wind m/s | On/Offshore wind +/- m/s |
|---|---|---|---|---|---|---|---|---|---|---|
| 11 | 6.80 | 4.1 | 2.70 | 83 | 277.8 | 8 | 225 | 125 | 4.12 | -2.36 |
| 82 | 6.40 | 4.2 | 2.20 | 86 | 278.1 | 9 | 237 | 113 | 4.63 | -1.81 |
| 98 | 6.30 | 4.00 | 2.30 | 85 | 278.1 | 10 | 240 | 110 | 5.14 | -1.76 |
| 235 | 5.20 | 2.30 | 2.90 | 82 | 278.4 | 14 | 235 | 115 | 7.20 | -3.04 |
| 408 | 3.80 | 0.40 | 3.40 | 78 | 278.6 | 15 | 243 | 107 | 7.72 | -2.26 |
| 868 | 2.60 | -16.40 | 19.00 | 23 | 282.0 | 17 | 265 | 85 | 8.75 | 0.76 |
| 1107 | 1.20 | -23.80 | 25.00 | 14 | 282.9 | 18 | 269 | 81 | 9.26 | 1.45 |
| 1269 | 0.00 | -18.00 | 18.00 | 24 | 283.3 | 19 | 273 | 77 | 9.77 | 2.20 |
| 1397 | -0.60 | -21.80 | 21.20 | 18 | 284.0 | 19 | 275 | 75 | 9.77 | 2.53 |
| 1546 | -1.30 | -26.30 | 25.00 | 13 | 284.8 | 21 | 285 | 65 | 10.80 | 4.57 |
| 1688 | -1.30 | -43.30 | 42.00 | 2 | 286.2 | 23 | 298 | 52 | 11.83 | 7.28 |
| 1707 | -1.40 | -43.40 | 42.00 | 2 | 286.4 | 23 | 300 | 50 | 11.83 | 7.61 |
| 2108 | -2.50 | -45.50 | 43.00 | 2 | 289.3 | 29 | 300 | 50 | 14.92 | 9.59 |
| 2219 | -3.10 | -11.10 | 8.00 | 54 | 289.8 | 30 | 300 | 50 | 15.43 | 9.92 |
| 2414 | -4.10 | -17.10 | 13.00 | 36 | 290.8 | 32 | 300 | 50 | 16.46 | 10.58 |
| 2455 | -4.30 | -13.90 | 9.60 | 47 | 291.0 | 33 | 300 | 50 | 16.98 | 10.91 |
| 2486 | -4.50 | -11.50 | 7.00 | 58 | 291.1 | 33 | 300 | 50 | 16.98 | 10.91 |
| 2655 | -5.50 | -43.50 | 38.00 | 3 | 291.8 | 32 | 302 | 48 | 16.46 | 11.02 |
| 2772 | -5.90 | -13.90 | 8.00 | 53 | 292.6 | 31 | 303 | 47 | 15.95 | 10.88 |
| 2815 | -5.90 | -22.90 | 17.00 | 25 | 293.1 | 31 | 303 | 47 | 15.95 | 10.88 |
| 2935 | -6.70 | -18.70 | 12.00 | 38 | 293.5 | 30 | 304 | 46 | 15.43 | 10.72 |
| 3046 | -6.50 | -49.50 | 43.00 | 2 | 294.9 | 29 | 305 | 45 | 14.92 | 10.55 |
| 3079 | -6.70 | -48.70 | 42.00 | 2 | 295.0 | 29 | 305 | 45 | 14.92 | 10.55 |
| 3237 | -7.10 | -40.60 | 33.50 | 5 | 296.3 | 29 | 305 | 45 | 14.92 | 10.55 |
| 3374 | -7.50 | -33.50 | 26.00 | 10 | 297.4 | 31 | 301 | 49 | 15.95 | 10.46 |
| 3503 | -8.10 | -16.10 | 8.00 | 53 | 298.1 | 33 | 298 | 52 | 16.98 | 10.45 |
| 3538 | -8.10 | -26.10 | 18.00 | 22 | 298.5 | 34 | 297 | 53 | 17.49 | 10.53 |
| 3585 | -8.10 | -42.10 | 34.00 | 5 | 299.0 | 35 | 296 | 54 | 18.01 | 10.58 |
| 3609 | -8.20 | -41.60 | 33.40 | 5 | 299.1 | 35 | 295 | 55 | 18.01 | 10.33 |
| 3826 | -8.90 | -36.90 | 28.00 | 8 | 300.7 | 37 | 308 | 42 | 19.03 | 14.15 |
| 3862 | -9.00 | -29.50 | 20.50 | 17 | 301.0 | 37 | 310 | 40 | 19.03 | 14.58 |
| 3899 | -9.10 | -22.10 | 13.00 | 34 | 301.3 | 37 | 309 | 41 | 19.03 | 14.37 |
| 4061 | -9.30 | -27.30 | 18.00 | 22 | 302.9 | 38 | 305 | 45 | 19.55 | 13.82 |
| 4149 | -10.10 | -15.10 | 5.00 | 67 | 302.9 | 38 | 302 | 48 | 19.55 | 13.08 |
| 4213 | -9.30 | -11.70 | 2.40 | 83 | 304.6 | 39 | 300 | 50 | 20.06 | 12.90 |
| 4225 | -9.30 | -11.80 | 2.50 | 82 | 304.8 | 39 | 300 | 50 | 20.06 | 12.90 |
| 4316 | -9.10 | -12.40 | 3.30 | 77 | 306.0 | 38 | 303 | 47 | 19.55 | 13.33 |
| 4367 | -9.40 | -12.70 | 3.30 | 77 | 306.2 | 37 | 305 | 45 | 19.03 | 13.46 |
| 5084 | -13.60 | -16.90 | 3.30 | 77 | 309.5 | 51 | 315 | 35 | 26.24 | 21.49 |
| 5506 | -16.10 | -19.30 | 3.20 | 76 | 311.4 | 49 | 315 | 35 | 25.21 | 20.65 |
| 5670 | -17.50 | -20.40 | 2.90 | 78 | 311.6 | 49 | 315 | 35 | 25.21 | 20.65 |
| 6687 | -25.00 | -28.20 | 3.20 | 75 | 314.8 | 52 | 310 | 40 | 26.75 | 20.49 |
| 7300 | -29.50 | -32.90 | 3.40 | 72 | 316.6 | 54 | 320 | 30 | 27.78 | 24.06 |
| 7571 | -31.50 | -35.20 | 3.70 | 70 | 317.4 | 54 | 322 | 28 | 27.78 | 24.53 |
| 8116 | -36.00 | -40.40 | 4.40 | 64 | 318.6 | 52 | 325 | 25 | 26.75 | 24.24 |
| 8375 | -38.10 | -42.80 | 4.70 | 61 | 310.1 | 54 | 325 | 25 | 27.78 | 25.18 |
| 9290 | -45.70 | -49.80 | 4.10 | 63 | 320.8 | 60 | 325 | 25 | 30.87 | 27.97 |

## Appendix
## Waves ahead of a Warm Front

An investigation by Wallington [1] showed that lee waves were likely to be significant in two zones ahead of a well-marked surface warm front. For the warm front investigated, lee waves were calculated and observed to be particularly pronounced at low levels in a zone between about 220 and 400 km ahead of the surface front's position. Pronounced lee wave flow was also possible at both high and low levels at distances between about 810 and 690 km ahead of the front. Between these zones short lee waves were possible, but their amplitudes would not be significant. As the warm front approaches both the amplitude and wavelength (max. 16.5 km) increase, as shown in Fig. 11.

In this 3-layer model the Scorer parameter $\ell_s$ for the stable layer is constant. In reality this parameter decreases as the wind-speed increases with altitude, in which case the upper wavelengths would be greater than the lower ones. Areas of warm frontal cloud can be seen on all the satellite pictures.

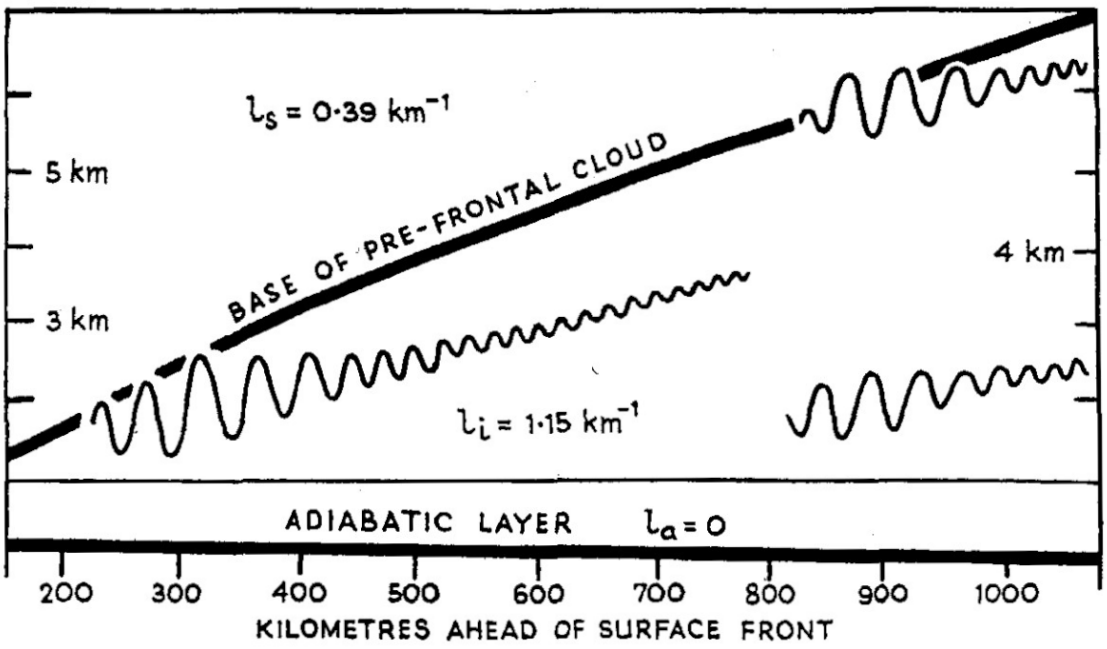


**Fig. 11: Waves ahead of a Warm Front. Adapted with permission from Wallington [1].**